

Dynamics of silver ions in $(\text{AgI})_x-(\text{Ag}_2\text{O}-n\text{B}_2\text{O}_3)_{1-x}$ glasses: A ^{109}Ag nuclear magnetic resonance study

S. H. Chung, K. R. Jeffrey, and J. R. Stevens

The Guelph-Waterloo Program for Physics, Guelph Campus, University of Guelph, Guelph, Ontario, Canada N1G 2W1

L. Börjesson

The Department of Physics, Chalmers University of Technology, Gothenburg, Sweden

(Received 4 October 1989)

Glasses having the composition $(\text{AgI})_x-(\text{Ag}_2\text{O}-n\text{B}_2\text{O}_3)_{1-x}$, where x is in the range from 0 to 0.7 and n is either 1 or 2, have conductivities as high as 10^{-2} S/cm at room temperature. NMR line-shape and spin-lattice-relaxation times have been measured for a range of compositions over the temperature region from -120 to 170°C in an attempt to test the predictions of various models for the dynamics of the Ag^+ ions. The line shapes are Lorentzian except at very low temperatures, where they were determined to be Gaussian. The linewidths were observed to decrease with increasing temperature, and no evidence for two Ag^+ populations was found. The spin-lattice-relaxation data feature a very broad T_1 minimum as a function of inverse temperature. Order-of-magnitude calculations suggest that the chemical shift interaction is responsible for the relaxation. Analysis using a single hopping rate for Ag^+ -ion migration does not fit the data. We have analyzed the data in terms of the empirical stretched exponential model and have found the resulting parameters to be in good agreement with the conductivity data.

INTRODUCTION

There is now a wide interest in studying fast ionic conductors as systems for research on mass transport in solid materials as well as for possible application to battery and fuel-cell technology. During the past decade much attention has been focused on metal halide salt-doped network glasses, since they offer extraordinary high room-temperature ionic conductivities, up to 10^{-2} Scm^{-1} . Moreover, the physical properties can easily be varied over large intervals by changing the chemical composition. Particular materials can be designed for specific applications as well as for studies of fundamental properties of disordered systems. Commonly, fast-ion conducting glasses are formed by an oxide glass former (e.g., B_2O_3 , P_2O_5 , SiO_2 , or GeO_2) which together with network modifiers (e.g., Ag_2O , Li_2O or Na_2O) can dissolve metal halide salts as dopants (e.g., AgI , LiI , LiCl , etc.).

The fast-ion conducting system $(\text{AgI})_x-(\text{Ag}_2\text{O}-n\text{B}_2\text{O}_3)_{1-x}$ comprises some of the best conducting glasses produced so far and is also a model system for studies of the conduction mechanism in vitreous electrolytes.¹⁻¹⁰ The addition of Ag_2O to B_2O_3 modifies the boron-oxygen network by changing the coordination number of some of the boron atoms from three to four. Depending on the value of n the number of BO_4 units increases at the expense of the number of BO_3 units and this conversion enables the glassy matrix to dissolve the AgI salt.¹⁰⁻¹³

Highly disordered electrolytes, such as the silver borate glasses, are an especially challenging area of research because the disorder far exceeds that found in crystalline fast-ionic conductors. In crystalline electrolytes, there is

a framework which exhibits a regular array while the mobile ions are disordered over many available sites. By contrast, in glasses there is no long-range order of any type. In studies of the mechanism for the high room-temperature conductivity ($\approx 10^{-2}$ Scm^{-1}),² interest has focused on the dynamics of the silver cations. A continuing controversy¹⁴ exists as to the microscopic picture of this motion. The controversy is centered on whether the glass is (1) homogeneous down to the distance scale of a few atomic spacings and the ions hop through a number of available sites in an immobilized disordered network or (2) inhomogeneous on the scale of 10 – 100 Å and conduction is a percolative process through α - AgI clusters. There is, presently, a trend to favor a picture of interconnected small (~ 8 – 10 Å) domains^{9,10} of distorted Ag-I-Ag-I units which provide conducting pathways for the silver ions undergoing some kind of jump diffusion.¹⁵

Previous NMR studies^{3,4} have recognized the capability of magnetic resonance to (a) discriminate amongst different silver environments because of the large chemical-shift range of silver ($\sim 10^3$ ppm) and (b) to attain unique information about the microscopic dynamics of ion transport through line-narrowing and spin-lattice-relaxation studies.

Villa *et al.*³ have chosen to investigate the dynamics by studying the relationship between composition and isotropic chemical shifts in AgI -doped silver borate glass. Their experiments were performed at relatively high temperatures (-70 – 124°C) where the rapid motion of ^{109}Ag averages out both the chemical-shift anisotropy and the distribution of isotropic chemical shifts. Low-temperature magic-angle spinning NMR experiments which would yield the latter while suppressing the former were not carried out for technical reasons. They also ob-

tained structural information for the doped glasses by analyzing the composition dependence of the average chemical shift, since a single motionally narrowed line was observed. They argued that their results rule out AgI microdomains and they cited the X-ray diffraction studies of Licheri *et al.*⁵ in support. However, Licheri *et al.* allow for the possibility of Ag-I-Ag aggregates of small dimensions.

Martin *et al.*⁴ have measured ¹⁰⁹Ag NMR linewidths and spin-lattice-relaxation times in AgI-doped silver borate glasses for temperatures between -120 and 230°C. They have used the simplest form of analysis which is to assume a single exponential correlation function to describe the ionic diffusion [Bloembergen-Purcell-Pound (BPP) theory].¹⁶ They conclude from their analysis of NMR linewidths and intensities that at low temperatures at least two types of Ag⁺ ions can be distinguished with respect to their mobility; one type being stationary on the NMR time scale, the other type performing fast-ion diffusion. At high temperatures they conclude that all cations appear to be mobile with local motions having activation energies of about 0.10 eV. In a recent publication, however, the authors state that upon reinspection, the Ag NMR relaxation data do not follow the expected BPP behavior.¹⁷

There are now many instances recorded in the literature where the simple BPP theory has been shown to be inappropriate as a description of NMR relaxation in fast-ionic conductors.¹⁸⁻²¹ Specifically, there are examples where (1) the frequency dependence of the minimum of the spin-lattice-relaxation time T_1 is less than expected,²² (2) there is an unexpected asymmetry in the slope of T_1 versus inverse temperature on the two sides of the minimum,¹⁷ (3) the spin-spin relaxation time T_2 dependence on temperature has more structure than expected,⁴ (4) the activation energies calculated from NMR studies are much smaller than those obtained from dc conductivity measurements,^{23,24} and (5) the prefactors in the Arrhenius expression for the correlation time describing the hopping motion are anomalously low.⁴ Non-BPP relaxation is believed to be the result of either the inherent non-random motion of the mobile ions which might arise if the movement of the ions is correlated²⁵ or within the entire population of mobile ions there are subgroups each of which have motion that is characterized by a BPP spectral density function but each described by a different correlation time.²⁶ The correlated motion of the ions resulting from the Coulomb interaction between them is the basis of the theory put forward by Funke.²⁵ Nonexponential correlation functions are also found when the structure of the fast-ionic conductor is such that the ionic diffusion has a dimensionality of one or two.²⁷ β -eucryptite (LiAlSiO₄)²⁸ and Na β -alumina²⁹ are examples of one- and two-dimensional ionic conductors which exhibit anomalous relaxation behavior.

In amorphous materials, a broad distribution of microscopic kinetic parameters are expected to occur and nonexponential mechanical and electrical relaxation appears to be the norm rather than the exception.³⁰ One approach is to assume a distribution of correlation times. An excellent discussion of many possible distribution

functions that have been used in fitting nuclear relaxation time data can be found in the paper by Beckmann.²⁶ For example, a Cole-Davidson distribution of correlation times has been shown to adequately fit the ⁷Li NMR data in a variety of glasses.³¹ A slightly different approach is to modify the correlation function describing the atomic motion. In particular, the stretched exponential form of the correlation function

$$g(t) = \exp[-(t/\tau)^\beta] \quad (1)$$

has been shown to be a more common phenomenon in amorphous materials than the Debye behavior ($\beta=1$). Kohlrausch³² first suggested the use of the stretched exponential form to describe viscoelasticity while Williams and Watts introduced the same equation for dielectric relaxation.³³ Jonscher³⁴ first pointed out the evidence for its remarkable universality. Subsequently, Ngai^{35,36} has demonstrated that the results of a large number of physical measurements of low-frequency fluctuation, dissipation, and relaxation phenomena in amorphous solids exhibit non-Debye behavior. While the stretched exponential function [Eq. (1)] was introduced as an empirical relation to explain experimental data there have been a number of attempts to provide a theoretical basis for its use.^{37,38} Villa and Bjorkstam^{39,40} advocate using the empirical Kohlrausch-Williams-Watts (KWW) correlation function [Eq. (1)] in a consistent manner to analyze the NMR linewidth and relaxation time data.

Present theories of motional narrowing and spin-lattice relaxation in amorphous fast-ionic conducting materials can only be rigorously tested with extremely high quality data. The investigations of Villa *et al.*³ and Martin *et al.*⁴ are limited by the experimental uncertainty in their data (the signal-to-noise ratio for Ag NMR is poor). In this study we report new careful linewidth and spin-lattice-relaxation measurements on (AgI)_x-(Ag₂O- n B₂O₃)_{1-x} systems for $n=1$ and 2 glasses. The data presented in this paper show the non-BPP type of behavior common in amorphous materials. This behavior was to be expected since previous mechanical and electrical relaxation results^{2,6,8} have shown that the relaxation function describing the ionic diffusion is highly nonexponential.

We have analyzed the data in terms of a non-BPP model using a stretched exponential. We believe that the quality of the experimental results and this approach for analyzing the data will resolve some of the previous ambiguities of NMR reports on AgI-doped borate glasses. Our analyses find agreement with conductivity data^{1,2} as predicted by Richards.²¹

THEORY

The basic theory of NMR as applied to fast-ionic conductors can be found in the review by Richards.²¹ Expressions have been developed for the spin-lattice and spin-spin relaxation times when the dominant nuclear spin interaction is one of the following: the dipolar interaction between like spins, the nuclear quadrupole interaction or dipolar interaction between unlike spins (in particular coupling with a paramagnetic impurity). For

Ag NMR in solids, the chemical-shift interaction is important^{4,17,41,42} and a brief derivation of the spin-lattice and spin-spin relaxation times is given below following the notation used by Richards.²¹

The Hamiltonian describing the chemical shift can be written

$$H = \sum_{\alpha} H_{\alpha}(t) = \sum_{\alpha=0,\pm 1} \sum_i \gamma h I_{i\alpha} A_{i\alpha}(t) B_0. \quad (2)$$

The applied magnetic field is B_0 , the Ag nuclei are labeled by i and

$$I_0 = I_z, \quad I_{\pm 1} = I_x \pm i I_y.$$

In general the chemical-shift tensor $A_{i\alpha\beta}$ ($\beta=0$ since the applied field defines the z direction) experienced by spin i varies in time as the ion moves from site to site throughout the glass. To take account of the motion of the ion let

$$A_{i\alpha}(t) = \sum_{\mu} n_{i\mu}(t) A_{\mu\alpha},$$

where

$$n_{i\mu}(t) = 1 \text{ if site } \mu \text{ is occupied by spin } i \text{ at time } t \\ = 0 \text{ otherwise.}$$

The spin-lattice relaxation rate is given by

$$\frac{1}{T_1} = (4\omega_0^2/N) \int_0^{\infty} \sum_{i\mu\mu'} n_{i\mu}(t) n_{i\mu'}(0) A_{\mu+1} A_{\mu'-1} \\ \times \exp(-i\omega_0 t) dt. \quad (3)$$

$$= 2 \langle \omega_i^2 \rangle \int g(t) \exp(-i\omega_0 t) dt \quad (4)$$

$$= 2 \langle \omega_i^2 \rangle J(\omega_0) \quad (5)$$

and the spin-spin relaxation rate by

$$\frac{1}{T_2} = \frac{1}{2T_1} + (2\omega_0^2/N) \int_0^{\infty} \sum_{i\mu\mu'} n_{i\mu}(t) n_{i\mu'}(0) A_{\mu 0} A_{\mu' 0} dt. \quad (6)$$

$$= \frac{1}{2T_1} + \langle \omega_i^2 \rangle \int g(t) dt \quad (7)$$

$$= \langle \omega_i^2 \rangle J(\omega_0) + \langle \omega_i^2 \rangle J(0). \quad (8)$$

The equation for $1/T_1$ is valid provided the correlation time τ_c describing the hopping motion of the Ag^+ ions is much shorter than T_1 . This condition is fulfilled except at very low temperatures. At low temperatures, the linewidth reaches a limiting value when the motion of the Ag^+ ions ceases. Often the static local fields result in frequencies having a temperature-independent Gaussian distribution with second moment $\langle \omega_i^2 \rangle$. In addition, the relation for T_2 is only valid in the extreme narrowing regime when the line shape is truly Lorentzian. The motionally narrowed half width at half maximum (HWHM) linewidth is given by

$$\Delta_{\text{LW}} = 1/2\pi T_2. \quad (9)$$

Bjorkstam *et al.*⁴⁰ have pointed out that a boundary can

be defined when the linewidth reaches half the static value. Kubo and Tomita⁴³ define the correlation time τ_c as the time integral of the correlation function

$$\tau_c = \int g(t) dt \quad (10)$$

so that the second term for $1/T_2$ in Eq. (6), the so-called adiabatic term,⁴⁴ can be written as $\langle \omega_i^2 \rangle \tau_c$. This term dominates at low temperatures but when the fluctuation rate of the local fields becomes of the order of the resonance frequency, the nonadiabatic effects must be taken into account. Now the lifetimes of the spin states become important and consequently the additional line broadening $1/2T_1$ must be considered. Notice from Eq. (5) that T_1 depends on the fluctuation in the component of the local field perpendicular to the applied field while the adiabatic part of T_2 depends on the fluctuations in the parallel component.

In a fast ionic conductor it is the dynamics of the diffusing ions which causes the fluctuations in the local fields and these are described in terms of the correlation function, $g(t)$ or the spectral density function, $J(\omega)$. The interpretation of the resulting correlation time depends on the form of the correlation function.^{16,26} For example, when the correlation function is a single exponential decay,

$$g(t) = \exp(-t/\tau_c), \quad (11)$$

the spectral density function

$$J(\omega) = \tau_c / (1 + \omega^2 \tau_c^2) \quad (12)$$

has the Debye behavior which is a single Lorentzian function of frequency. The resulting expressions for the relaxation times are given by

$$1/T_1 = 2 \langle \omega_i^2 \rangle \tau_c / (1 + \omega_0^2 \tau_c^2) \quad (13)$$

and

$$1/T_2 = \langle \omega_i^2 \rangle \tau_c + 1/2T_1. \quad (14)$$

For systems with a rate activated process the correlation time τ_c can be expressed in terms of a prefactor τ_{∞} and the activation energy E_A .

$$\tau_c = \tau_{\infty} \exp(E_A/kT), \quad (15)$$

where T is the temperature and k Boltzmann's constant. Equation (13) predicts a minimum in T_1 when $\omega_0 \tau_c = 1$ and the value of $T_{1 \text{ min}} = \omega_0 / \langle \omega_i^2 \rangle$. For the chemical-shift interaction, $T_{1 \text{ min}} \propto \omega_0^{-1}$. On the low-temperature side ($\omega_0 \tau_c \gg 1$) of the minimum $T_1 \propto \tau_c$ and independent of frequency. On the high-temperature side ($\omega_0 \tau_c \ll 1$) there is a frequency dependence; $1/T_1 \propto \omega_0^2 \tau_c$.

As was discussed in the Introduction it has been shown that this formulation of nuclear-spin relaxation, known as the BPP theory,¹⁶ does not fit the details of the experimental data for fast ionic conductors. The KWW form for the correlation function [Eq. (1)] predicts the following adiabatic linewidth

$$\Delta_{\text{LW}} = (1/2\pi\beta) \langle \omega_i^2 \rangle \Gamma(1/\beta) \tau_{\infty} \exp(E_A/kT), \quad (16)$$

where Γ is the gamma function. The spectral density function needed for the determination of T_1 must be calculated numerically from the correlation function given in Eq. (1).⁴⁵

In the modified Debye-Hückel theory put forward by Funke,^{46,47} the mobile ions occupy a number of similar sites throughout the sample. Because of their mutual repulsion, these ions tend to stay as far apart as possible. The single-particle potential seen by each ion is made up of two contributions: the potential due to the structure of the glass and the "Coulomb potential" resulting from neighboring ions. The effective potential is characterized by two parameters Δ and δ . If the ion is thermally activated to move from site A to site B two subsequent events can occur: (1) the ion can hop back into site A or (2) the ion can remain in site B with the surrounding ions adjusting their positions in response to the original movement with the result that the Coulomb minimum is shifted towards site B . Funke made the reasonable assumption that the correlation function $g(t)$ needed for NMR relaxation times can be approximated by the probability $W_A(t)$ of finding the ion at site A at time t provided it was there at $t=0$. The corresponding spectral density function is

$$J(\omega) = \text{Re} \int_0^\infty W_A(t) \exp(-i\omega t) dt \quad \text{with } W_A(0) = 1. \quad (17)$$

Funke showed that

$$J(\omega) = \Gamma^{-1} / \{ 1 + [\omega \Gamma^{-1} + \Phi''(\omega) / \Phi'(\omega)]^2 \}, \quad (18)$$

$$\Gamma = \Gamma_0 \Phi'(\omega). \quad (19)$$

It is assumed that

$$\Gamma_0^{-1} = \tau_\infty \exp(\Delta/kT). \quad (20)$$

The normalized frequency function

$$\Phi(\omega) = \Phi'(\omega) + i\Phi''(\omega) \quad (21)$$

is defined in terms of the probability $W(t)$ of a back jump not occurring:

$$\Phi(\omega) - \Phi'(0) = i\omega \int_0^\infty [W(t) - W(\infty)] \exp(-i\omega t) dt. \quad (22)$$

The quantity $W(t)$ is a complex function of the well-depth parameters Δ and δ . There are two special cases which are of interest to NMR studies. The BPP theory is recovered when $W(t) = W(\infty)$ and $J(0) = [\Gamma_0 \Phi(0)]^{-1}$ determine the adiabatic linewidth.

$$\begin{aligned} \Delta_{LW} &= (1/2\pi) \langle \omega_l^2 \rangle J(0) \\ &= (1/2\pi) \langle \omega_l^2 \rangle \tau_\infty \exp[(3\Delta - 2\delta)/kT], \end{aligned} \quad (23)$$

where the factor $(3\Delta - 2\delta)$ is the expected low-frequency activation energy. Again, the expression for $1/T_1$ must be calculated numerically.

SAMPLE PREPARATION AND EXPERIMENTAL TECHNIQUE

For the preparation of the (AgI)_x-(Ag₂O- n B₂O₃)_{1-x} systems for $n=1$ and $n=2$ glasses, 30 g batches of stoichiometric amounts of high purity, water-free AgNO₃, B₂O₃, and AgI powders were thoroughly milled and mixed. The powder mixtures were then fused in alumina crucibles at 700–750 °C until complete gas removal, i.e., about 40 min. The melts were then homogeneous and the color was dark red. Cylindrical glass samples, 7 mm in diameter and 10 mm high, were formed by casting the melt into a stainless steel mold held at 100 °C. The samples which were homogeneously red to orange in color, transparent and of good optical quality, were then annealed for three h at 30 °C below the glass transition temperature T_g (~280 °C). Throughout this paper the composition of the samples will be referred to by their x and n values and denoted as (x, n) .

The NMR spectrometer used in these experiments is a "home-built" instrument featuring a wideband transistorized 300 w transmitter and narrow band GaAs FET preamplifiers tuned for each nuclear resonance frequency. The spectrometer was used with a Brüker 6.3 T or an Oxford Instruments 8.5 T superconducting magnet. In these fields the ¹⁰⁹Ag resonance occurs at 12.528 and 16.763 MHz. The data acquisition was via a Nicolet Explorer digital oscilloscope interfaced to an IBM/PC. The computer was programed for automatic temperature control and data acquisition.

At all but the very lowest temperatures, the NMR spectra were obtained by collecting the free induction decay (FID) following a single $\pi/2$ pulse and Fourier transforming the data. There was some distortion of the spectra because of the recovery time of the receiver following the radio-frequency (rf) pulse from the transmitter which was approximately 30 μ s. This large recovery time was the result of using a high- Q (~120) coil in order to maximize the signal-to-noise ratio and the low resonance frequency for ¹⁰⁹Ag.

Each sample at a sufficiently low temperature produced a nuclear-spin echo signal following a $\pi/2$ - τ - π pulse sequence. The echo was digitized and the signal starting at the peak of the echo was Fourier transformed to produce an echo spectrum.

The spin-lattice-relaxation time, T_1 , was determined by sampling the amplitude of the FID following the $\pi/2$ pulse in the π - τ - $\pi/2$ sequence for about 15 values of τ .

The NMR probe was designed to have the sample surrounded by a thick-walled copper container whose temperature was electronically regulated to ± 0.1 °C over the course of the data acquisition for a spectrum or T_1 measurement. A copper-constantan thermocouple located near the sample was used to record the actual sample temperature which was known to ± 0.5 °C.

RESULTS

Line shape

The behavior of the ¹⁰⁹Ag NMR line shape for each sample may be divided into two separate temperature re-

gions. At high temperature the NMR line shape was motionally narrowed and could be accurately fit with a Lorentzian line shape. Following the exponential FID, no echo signal could be found with a refocusing π pulse. At low temperature the FID becomes so rapid that the signal was lost in the receiver recovery time. In this same temperature region an echo signal could be observed. Figure 1 shows representative spectra for the (0.5,1) sample obtained from the FID at 12.5 MHz. At the highest temperature available with the existing NMR probe, 170°C, the linewidth was about 30 Hz while at -120°C it has increased to approximately 10 kHz. The poor baseline and signal-to-noise ratio at the lowest temperature in Fig. 1 result from a loss of signal in the receiver recovery time.

A typical fit to the motionally narrowed line is shown in Fig. 2. The Lorentzian line shape fits the data very well and the half-width at half-maximum amplitude (Δ_{LW}) is a very well-defined parameter in terms of the spin-spin relaxation time (T_2) since

$$\Delta_{LW} = 1/2\pi T_2 \quad (24)$$

The Lorentzian linewidth is shown as a function of the

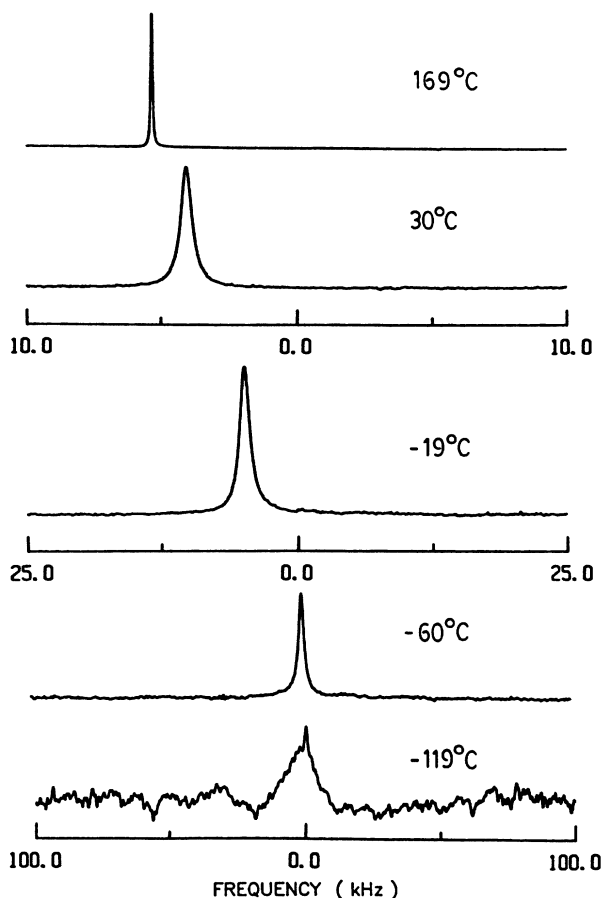


FIG. 1. ^{109}Ag NMR spectra from the (0.5,1) sample obtained by Fourier transforming the FID signal following a single $\pi/2$ pulse. The line is motionally narrowed with increasing temperature.

reciprocal temperature for each of the samples in Fig. 3. For the data that are shown the linewidths are less than 1 kHz and the line shapes are well represented by a Lorentzian. Below 1 kHz the lines are completely motionally narrowed and the crossover to a Gaussian line shape at low temperatures has not begun. In the region where the linewidth was less than 1 kHz and the temperature is below that of the T_1 minimum, the adiabatic term in the expression for the linewidth is dominant and there is a roughly Arrhenius temperature dependence for each sample. The average ratio of the T_2 values at the two frequencies 16.8 and 12.5 MHz for all of the samples was found to be 1.44 ± 0.08 . This ratio can be compared with the ratio of the resonance frequencies which is 1.33 or the frequencies squared which is 1.77. Table I lists the activation energies derived directly from least-squares fits of the data to the equation

$$\Delta_{LW} = A \exp(E_A/kT), \quad (25)$$

where A is an amplitude factor. The fitting was only carried out on the data in the adiabatic region. The linewidth increases with magnetic field but the activation energies are independent of field within experimental error.

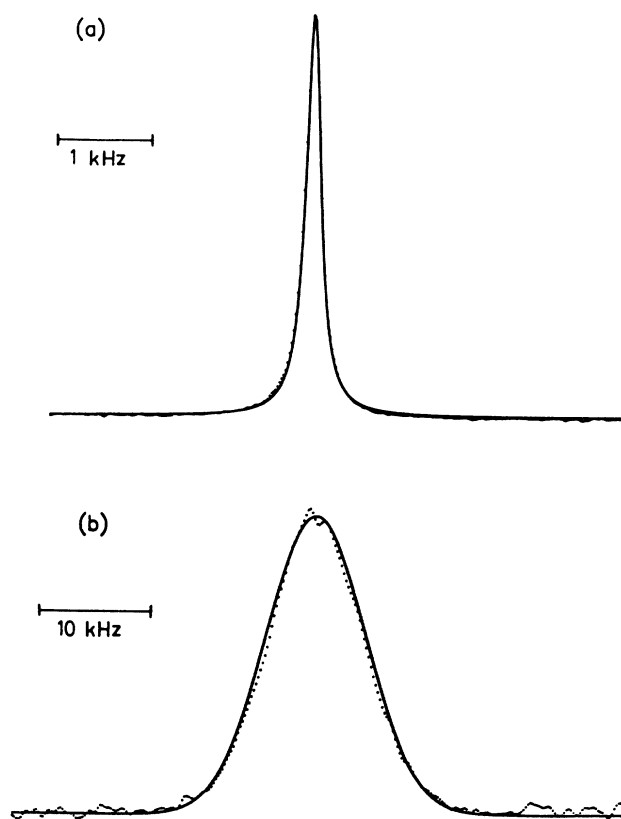


FIG. 2. The upper spectrum (dots) is for the (0.5,1) sample at 89.5°C and 16.8 MHz. The fitted Lorentzian curve (solid line) has a half width at half maximum linewidth of 89 Hz. The lower spectrum is for the same sample at the same frequency but at -99.3°C. The fitted Gaussian curve has a half-width at half maximum linewidth of 4.3 kHz.

TABLE I. Activation energies from the NMR linewidths.

Sample x	n	Resonance frequency (MHz)	Activation energy (eV)	Amplitude factor
0.7	1	12.5	0.10 ± 0.01	5.4×10^{-3}
		16.8	0.10	7.5
0.5	1	12.5	0.11	4.2
		16.8	0.12	5.1
0.6	2	12.5	0.093	19.3
		16.8	0.093	30.7
0.5	2	12.5	0.11	17.0
		16.8	0.10	33.2
0.3	2	12.5	0.15	15.9

At low temperatures when an echo signal was observed the line shape changed from being Lorentzian to Gaussian. Figure 2 shows a Gaussian fit for the (0.5,1) sample at 12.5 MHz at -99.3°C and clearly the fit is very good indicating the change from the Lorentzian high-temperature form. Figure 4 shows the low-temperature line shapes for several of the samples including results at the two resonance frequencies and Table II summarizes the linewidth parameters obtained by fitting the experimental data to a Gaussian curve. The linewidth reported in Table II for the (0.7,1) sample probably is not the max-

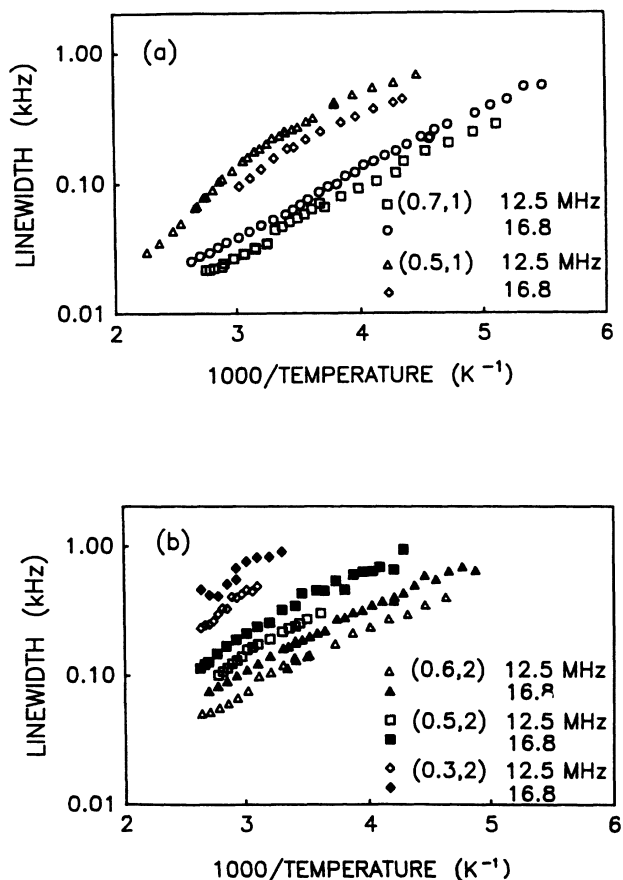


FIG. 3. The motionally (Lorentzian) narrowed linewidths are shown as a function of the reciprocal temperature for each of the samples investigated in this study.

TABLE II. Low-temperature Gaussian linewidth parameters.

Sample x	n	Resonance frequency (MHz)	Temperature ($^\circ\text{C}$)	Linewidth (HWHM) (kHz)
0.7	1	12.5	-117.8	2.5 ± 0.2
		16.8	-120.4	4.0
0.5	1	12.5	-60.7	3.2
		16.8	-59.7	4.5
0.6	2	12.5	-119.1	5.0
		16.8	-103.3	3.4
0	2.1	12.5	68.9	3.2

imum static width but lower temperatures were not possible with the present apparatus. Interestingly, there was a definite dependence of the linewidth on magnetic field but little variation between samples including the sample without AgI.

From the low-temperature Gaussian linewidth it is possible to determine the second moment, $\langle \omega_l^2 \rangle$ which is needed in the analysis of the motional narrowing at high temperature. A careful study was made of the line shape for the (0.5,1) sample down to -120°C . The width reached a maximum at -90°C and remained constant upon decreasing the temperature further. From the limiting low-temperature linewidth for this sample at 16.8 MHz it was found that $\langle \omega_l^2 \rangle = (7.0 \pm 0.4) \times 10^8 \text{ s}^{-2}$. From limited measurements on several samples it was determined that $\langle \omega_l^2 \rangle$ as determined from the low-temperature linewidth is proportional to ω_0^2 .

Spin-lattice relaxation

For each sample, at all the temperatures investigated in this study, the return of the nuclear magnetization to equilibrium was found to be exponential so that a unique

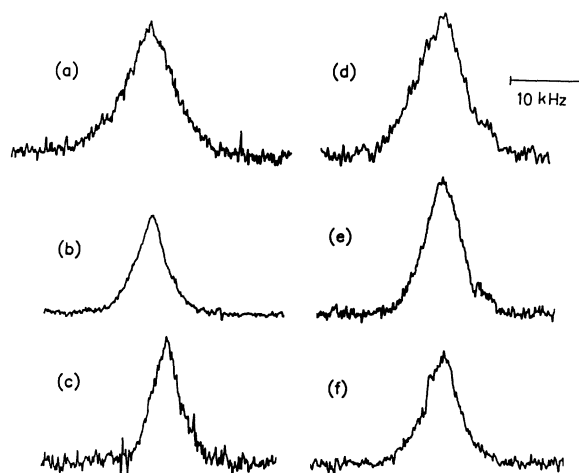


FIG. 4. ^{109}Ag NMR spectra are obtained by Fourier transforming the echo signal following a $\pi/2-\tau-\pi$ pulse sequence. (a) sample (0.7,1) at 16.8 MHz and -120.4°C ; (b) sample (0.7,1) at 12.5 MHz and -121.8°C ; (c) sample (0.2,1) at 12.5 MHz and 68.9°C ; (d) sample (0.5,1) at 16.8 MHz and -69.5°C ; (e) sample (0.5,1) at 12.5 MHz and -60.7°C ; (f) sample (0.6,2) at 12.5 MHz and -94.8°C .

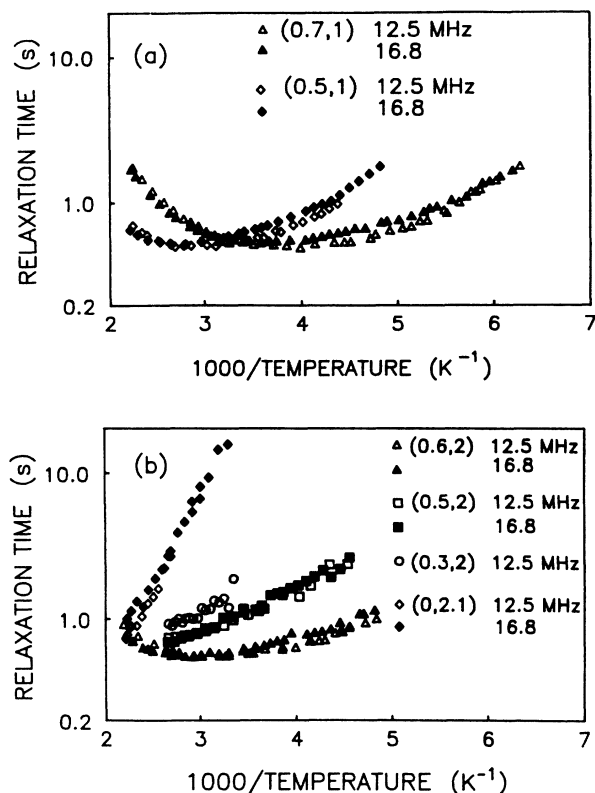


FIG. 5. ^{109}Ag nuclear spin-lattice-relaxation times as a function of reciprocal temperature.

T_1 could be assigned to each measurement. The error associated with each T_1 measurement is about $\pm 1\%$. The results for each sample are shown in Fig. 5 as a function of reciprocal temperature. A definite T_1 minimum is observed for the (0.7,1), (0.5,1), and (0.6,2) samples while the minimum for the other samples appears to occur at higher temperatures than could be reached with the present apparatus. There is a definite trend for the T_1 minima to move to lower temperature with increasing Ag^+ concentration in the sample. The T_1 minima are extremely broad and the frequency dependence of the relaxation is very weak on both sides of the T_1 minimum for all the samples.

DISCUSSION

The static linewidth

The static linewidth increases with the Larmor precessional frequency suggesting that the dominant spin interaction which determines the low-temperature static linewidth is the chemical shift. The powder pattern characteristic of a spectrum determined by the anisotropic part of the chemical shift is not seen but rather the line shape is fit very well by a Gaussian functional form. Because a glass is a heterogeneous system, there is expected to be a wide variety of Ag^+ sites in the amorphous glassy matrix. These results suggest that there is a wide distribution in the components of the chemical-shift tensor throughout the glass. The question arises as to whether

the broad low-temperature linewidth is simply a result of a wide distribution of isotropic chemical shifts or does the anisotropic part contribute as well.

Villa *et al.*³ have measured the average isotropic chemical shift (that is the center of the motionally narrowed NMR line) in a variety of silver borate glasses and have found that these can range from 200 to 800 ppm referenced to 10 M AgNO_3 . Becker and Von Goldammer⁴⁸ and Looser and Brinkman⁴⁹ have measured the isotropic chemical shifts in silver iodide, RbAg_4I_5 and KAg_4I_5 , finding that the shift was in the range of 700–800 ppm while Burges *et al.*⁵⁰ found that the Ag oxyanions have shifts ranging from 0 to -50 ppm. It may be expected, therefore, that the isotropic chemical shifts at the various sites in the silver borate glass will range over 800 ppm which could easily account for the observed Gaussian linewidths of 10 kHz [full width at half maximum (FWHM)] at 16.8 MHz (620 ppm). However, as Villa *et al.*³ have argued the (0,2,1) sample should only have $\text{BO}_4\text{-Ag-BO}_4$ type of units and the range of isotropic chemical shift should be minimal. Nevertheless, the low-temperature linewidth for this sample is very similar to that found for the highly AgI-doped samples. On the basis of this observation the anisotropic part of the chemical shift should be responsible for the static width, at least, in the (0,2,1) sample and probably makes a significant contribution in all of the samples.

The spin-lattice relaxation

There is no doubt that the silver ion diffusion causes the observed temperature dependence of both the linewidth and the spin-lattice-relaxation time. It is not clear, however, if the same nuclear spin interaction is responsible for temperature behavior of both the linewidth and T_1 . While it has been argued that the fluctuating fields due to motion of the Ag spins and the variety of chemical-shift tensors in the glass cause the observed narrowing of the NMR line, there are other possible processes which could influence the spin-lattice relaxation. Other possibilities include the Ag-I dipolar coupling, the Ag-I scalar interaction coupled with fast quadrupolar relaxation of the iodine spins, direct modulation of the scalar coupling between either the ^{109}Ag and ^{107}Ag spins or the ^{109}Ag and I spins by the ionic motion or the time-dependent pseudodipolar interaction between the Ag and neighboring I spins.

It has been argued in other studies of Ag spin-lattice relaxation that it is the time-dependent anisotropic chemical shift which is the dominant mechanism.^{4,17,41} An order of magnitude calculation indicates that the chemical shift must be considered in any analysis of T_1 . An estimate of the spin-lattice relaxation rate can be obtained by using the second moment of the static linewidth as a measure of the strength of the chemical-shift interaction. For purposes of estimating the value of T_1 at the minimum it is sufficient to let the spectral density, $J(\omega_0)$, in Eq. (5) have the simple Debye form $\tau_c / (1 + \omega_0^2 \tau_c^2)$. The predicted value of $T_{1\text{min}} = \omega_0 / \langle \omega_c^2 \rangle$. For the (0.7,1) sample at 16.8 MHz, the estimated values for $T_{1\text{min}}$ is 0.15 s while the experimental value is 0.49 s. The strength of the

chemical shielding interaction is definitely large enough to dominate the spin-lattice relaxation. The fact that the estimated value of $T_{1\text{ min}}$ is a factor of 3 smaller than the experimental value indicates that $\langle \omega_i^2 \rangle$ is about $\frac{1}{3}$ of $\langle \omega_i^2 \rangle$.

The dipolar interaction can be neglected on the basis of order of magnitude calculations of the possible contributions to T_1 . X-ray diffraction studies show that the nearest magnetic spin to a Ag^+ ion is an iodide ion 2.85 Å away.⁵ This dipolar interaction made time dependent by the Ag^+ motion would produce a $T_{1\text{ min}} \approx 1000$ s. An estimate of the influence of scalar relaxation of the second kind requires a knowledge of the scalar interaction between a Ag spin and the neighboring I spin, $J_{\text{Ag-I}}$, as well as the spin-spin relaxation time of the I spin τ_2 since

$$1/T_1 = (8\pi^2/3)J_{\text{Ag-I}}^2 S(S+1) \{ \tau_2 / [1 + (\omega_{\text{Ag}} - \omega_{\text{I}})^2 \tau_2^2] \} \quad (26)$$

and $S = \frac{5}{2}$ for iodine. Very little is known about Ag-I coupling constants but the Sn-I coupling constant in SnI_4 is known to be 940 Hz.⁵¹ Using 1000 Hz as an estimate of $J_{\text{Ag-I}}$, τ_2 would have to be less than 10^{-8} s to influence T_1 . In $\beta\text{-AgI}$, the $T_{1\text{ min}}$ for iodine is 60 μs ,⁵² so that it is unlikely that scalar coupling of the second kind makes a contribution to the observed T_1 .

Scalar coupling of the first kind may be significant. This interaction has the same form as Eq. (26) with τ_2 replaced by τ_c the correlation time for the ionic motion. Now the spin interaction is time dependent because the scalar coupling is modulated by the ionic motion. Now with the same value for $J_{\text{Ag-I}}$ the $T_{1\text{ min}}$ is predicted to be 20 s. If the coupling constant is somewhat larger than 1000 Hz this mechanism could influence the observed T_1 . There is also the possibility of scalar coupling between the two isotopes of silver causing relaxation as is often seen in thallium salts.^{53,54} To be an important effect the J parameter would have to be as large as it is in the thallium salts $\sim 5\text{--}10$ kHz.

On the basis of these arguments, it is reasonable to assume that the spin-lattice relaxation is dominated by the chemical-shift interaction and Eq. (5) is applicable. The form of the spectral density function depends on the correlation function used to describe the diffusion of the Ag^+ ions. In this paper the correlation functions for the BPP theory, the KWW expression and the theory put forward by Funke have been examined in detail. The temperature dependence of the thermally activated correlation time has been assumed to be given by Eq. (15).

We consider that the time τ_∞ in Eq. (15) is related to the average "rattling" time for a Ag^+ ion in a potential well before jumping. This cage rattling frequency has been observed to be between 50 and 150 cm^{-1} for silver borate glasses.⁵⁵ These frequencies correspond to times between 2 and 7×10^{-13} s.

Figure 6 shows least-squares fits to the data for the (0.7,1) samples at 12.5 MHz for the BPP, KWW, and Funke correlation functions. The least-squares fitting parameters for the three samples (0.7,1), (0.5,1), and (0.6,2) where there are data on both sides of the T_1 minimum

are presented in Table III for each model. In order to compare the quality of the various fits a fitting parameter has been defined

$$Q_F = \sum_i w_i (y_i - yf_i)^2 / \left[\sum_i w_i (y_i^2 + yf_i^2) \right]. \quad (27)$$

The experimental data points are y_i and the calculated values are yf_i . The data are weighted with the factors w_i which were taken to be proportional to $1/y_i^2$. This parameter varies between 0 and 1, with a smaller value indi-

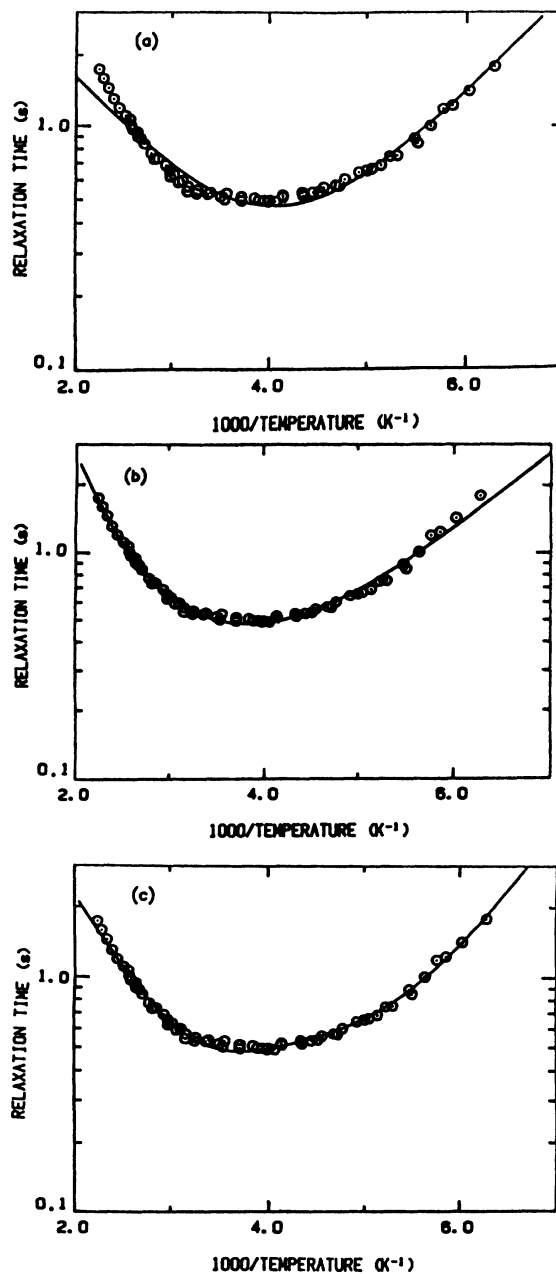


FIG. 6. The spin-lattice relaxation time data for the (0.7,1) sample at 12.5 MHz are shown as a function of reciprocal temperature. The solid line in each plot is a least-squares fit to the data using (a) the BPP theory, (b) the KWW empirical expression, and (c) the modified Debye-Hückel theory as proposed by Funke.

TABLE III. Fitting parameters for spin-lattice-relaxation time results.

Sample		Frequency (MHz)	BPP theory		τ_∞ (10^{-10} s)	Q_F (10^{-5})
x	n		$\langle \omega_l^2 \rangle$ (10^8 s $^{-2}$)	E_A (eV)		
0.7	1	12.5	1.17	0.083	1.6	5
		16.8	1.37	0.075	1.9	8
0.5	1	12.5	1.10	0.092	3.2	0.9
		16.8	1.38	0.083	3.9	1.4
0.6	2	12.5	0.98	0.075	4.4	1.4
		16.8	1.27	0.069	5.3	3

Sample		Frequency (MHz)	KWW theory		E_A (eV)	τ_∞ (10^{-14} s)	Q_F (10^{-5})
x	n		β	$\langle \omega_l^2 \rangle$ (10^8 s $^{-2}$)			
0.7	1	12.5	0.24	2.0	0.3	0.83	1.3
		16.8		2.4	0.29	1.35	1.5
0.5	1	12.5	0.28	1.7	0.3	1.6	0.4
		16.8		2.1	0.3	2.2	1.1
0.6	2	12.5	0.26	1.6	0.27	2.2	0.6
		16.8		2.1	0.27	3.5	2

Sample		Frequency (MHz)	Funke theory		δ (eV)	τ_∞ (10^{-10} s)	Q_F (10^{-5})
x	n		$\langle \omega_l^2 \rangle$ (10^8 s $^{-2}$)	Δ (eV)			
0.7	1	12.5	1.6	0.11	0.10	0.31	0.7
		16.8	2.0	0.11	0.094	0.25	1.1
0.5	1	12.5	1.5	0.13	0.12	0.53	1.7
		16.8	2.0	0.13	0.12	0.38	0.5
0.6	2	12.5	1.3	0.11	0.096	0.83	0.3
		16.8	1.9	0.11	0.10	0.45	1.1

cating a better fit.

The BPP theory does not fit the experimental data. The data are not symmetric with respect to the $T_{1 \min}$ on the plot shown in Fig. 6 as expected by the theory. There is no frequency dependence on the high-temperature side of the $T_{1 \min}$ whereas the theory predicts $1/T_1 \propto \omega_0^2$. In the BPP theory at the $T_{1 \min}$, $\omega_0 \tau_c = 1$. For the (0.6,2) sample the $T_{1 \min}$ occurs at 35°C; τ_c is predicted to be 1.3×10^{-8} s but Brillouin scattering and ultrasonic attenuation results show $\tau_c \approx 10^{-9}$ s at this same temperature.

From Table III it can be seen that for the T_1 data, the three-parameter BPP fit, and the four-parameter fit to the modified Debye-Hückel model due to Funke⁴⁶ give values of τ_∞ between two and three orders of magnitude slower

than the Ag^+ ion rattling period.

For the KWW fit to the T_1 data we first allowed four parameters ($\langle \omega_l^2 \rangle$, E_A , τ_∞ , β) to vary for the (0.7,1) sample since it comprised the largest data set. The integrals involved were numerically calculated using the method proposed by Dishon, Weiss, and Bendler.⁴⁵ We found acceptable fits for a range of β values between 0.22 and 0.28, with values of E_A of the order of 0.3 eV and τ_∞ values in the range from 10^{-13} to 10^{-15} s. It was recognized that the values of E_A were in agreement with the activation energies measured for these samples by dc conductivity (see Table IV). Further using the Einstein relation and assuming Fickian diffusion one can calculate values of τ_∞ from the conductivity data.³ These values are of the order of 10^{-13} s and are tabulated in Table IV.

TABLE IV. KWW fitting parameters for NMR spin-lattice-relaxation time and linewidth results compared to conductivity results.

Sample		Conductivity ^a		NMR			T_1		T_2	
x	n	E_A (eV)	τ_∞ (10^{-13} s)	Frequency (MHz)	β	$\langle \omega_l^2 \rangle$ (10^8 s $^{-2}$)	E_A (eV)	τ_∞ (10^{-13} s)	E_A' (eV)	τ_∞' (10^{-12} s)
0.7	1	0.23	2.6	12.5	0.26	1.8	0.29	0.22	0.10	1.6
				16.8	0.26	2.3	0.27	0.35	0.10	0.85
0.5	1	0.30	2.1	12.5	0.28	1.6	0.31	1.5	0.09	7.1
				16.8	0.28	2.1	0.31	1.9	0.10	4.3
0.6	2	0.27	2.7	12.5	0.26	1.6	0.27	2.0	0.09	3.0
				16.8	0.26	2.1	0.27	3.7	0.09	2.2

^aReference 2.

The values of E_A and τ_∞ listed in Table IV provide excellent fits to our T_1 data. These values were selected by constraining the values of τ_∞ to be in the 10^{-13} s range to agree with the infrared results.⁵⁵ The fits to the data, however, indicate that $\langle \omega_i^2 \rangle \propto \omega_0$.

Table III shows that the spin-lattice relaxation time data as a function of reciprocal temperature can be fit using a number of models. The BPP theory can be rejected on the basis of a much poorer fit than either the KWW or Funke expressions which fit the data equally well. We have also tried using the BPP approach but with two correlation times and expressions incorporating a Gaussian and a Fröhlich distribution of activation energies.^{6,56} These also give fits of the same quality as the KWW or Funke expressions. In all of the fits, except the KWW, activation energies or averages thereof were of the order of 0.1–0.15 eV and τ_∞ was of the order of 10^{-10} – 10^{-11} s. For the KWW fits with β in the range 0.26 to 0.28 we obtain activation energies of 0.3 eV and values of τ_∞ in the range of 10^{-13} s. The obtained β value of the (0.6,2) sample is in excellent agreement with recent low-temperature dielectric measurements which give a β value of 0.25.⁵⁷ However, previous electrical relaxation results gave $\beta=0.52$ from a fit to the imaginary part of the modulus spectrum.⁵⁸ Mechanical relaxation in the same frequency range gave a slightly larger β (0.35).⁸ Because the far infrared results on the types of glass which we are studying show absorption due to vibrations in the 50–150 cm^{-1} range,⁵¹ we suggest that τ_∞ be associated with the reciprocal of these frequencies. Given this assumption our T_1 results agree very well with the dc conductivity results of Chiodelli *et al.*² According to Richards²¹ such agreement between NMR T_1 results and dc conductivity indicates discrete, nearest neighbor, classical hopping where the attempt frequency corresponds to a measured optical phonon mode.

Motional narrowing of the linewidth

The diffusion of the Ag^+ ions through a variety of different sites in the glass means that the Ag nuclei experience fluctuating magnetic fields due to the different components of the chemical-shift tensor at each site. The theoretical predictions of the NMR linewidth given above in the theory section differ only in the choice of the correlation function used to describe the dynamics of the diffusing Ag^+ ions. Each of the theories, however, predicts an exponential increase in the linewidth as a function of the reciprocal of the temperature. The linewidth continues to increase as the temperature decreases until the static value is reached. The experimental behavior is only roughly exponential for some of the samples investigated as shown in Fig. 3. The most obvious deviation occurs with the (0.5,1) sample where the data appear to have two straight line segments.

The interpretation of the fitting parameters listed in Table I depends on the model chosen to describe the ionic diffusion. The equations given in this paper are only valid in the motionally narrowed region where the average correlation time is greater than the reciprocal of the Larmor precessional frequency. Operationally, this means that the adiabatic expressions should only be used to fit the data in the lower-temperature region below the T_1 minimum.

Using the KWW correlation function the linewidth is given by Eq. (16). In this equation it is assumed that $\langle \omega_i^2 \rangle$ has the same value as in the absence of motion and that the temperature dependence of the linewidth is Arrhenius. The parameters E'_A and τ'_∞ obtained from the T_2 experimental data are given in Table IV. Notice that the linewidth ($1/T_2$) data versus reciprocal temperature produce somewhat nonlinear graphs with the most nonlinear being for the (0.5,1) sample. In addition fitting to the KWW model produces activation energies which are about one third of those obtained from the T_1 data. We suggest that the assumption of a temperature-independent $\langle \omega_i^2 \rangle$ may be incorrect. If the bottom of the potential wells in which the Ag^+ ion can reside, have a distribution of energies, then the number of different sites being sampled by the ions increases with temperature. The range of chemical shifts will then be a function of temperature. Such a temperature dependence could result in both a higher average activation energy and be responsible for the observed nonlinearity in the Arrhenius plot. An increase with temperature of anharmonic effects was observed by Carini *et al.*⁵⁹ for these glasses from ultrasonic measurements. However, their observations indicate that anharmonicity cannot account for the increase in $\langle \omega_i^2 \rangle$ required to give average activation energies in the region of 0.3 eV for our linewidth measurements.

In conclusion we can make the following points. (1) Because a single NMR line is observed at all temperatures there is no evidence for two or more populations of Ag^+ ions. There is no evidence for a subdivision of ions into those nearest iodine atoms and those nearest oxygen atoms nor can the ions be divided into mobile and immobile species. (2) In our opinion the experimental NMR data are best fit using the empirical KWW model. The non-BPP-type behavior is a result of a variety of different silver ion sites having a range of potential well depths not the correlated silver ion motion proposed by Funke. (3) There are a number of unresolved problems with the present analysis. In particular, the frequency dependence of $\langle \omega_i^2 \rangle$ and $\langle \omega_i^2 \rangle$ as determined from the spin-lattice relaxation times is not proportional to ω_0^2 as expected. (4) The analysis of ^{109}Ag nuclear spin-relaxation time data in fast-ionic conductors is severely limited because so little is known about the chemical-shift tensor in silver compounds.

¹G. Chiodelli, A. Magistris, M. Villa, and J. L. Bjorkstam, *J. Non-Cryst. Solids* **51**, 143 (1982).

²G. Chiodelli, G. Campari-Vigano, G. Flor, A. Magistris, and M. Villa, *Solid State Ionics* **8**, 311 (1983).

³M. Villa, G. Chiodelli, A. Magistris, and G. Licheri, *J. Chem. Phys.* **85**, 2392 (1983).

⁴S. W. Martin, H. J. Bishoff, M. Mali, J. Roos, and D. Brinkmann, *Solid State Ionics* **18/19**, 421 (1986).

- ⁵G. Licheri, A. Musini, G. Paschina, G. Piccaluga, G. Pinna, and A. Magistris, *J. Chem. Phys.* **85**, 500 (1986).
- ⁶G. Carini, M. Cutroni, M. Federico, G. Galli, and G. Tripodo, *Phys. Rev. B* **30**, 7219 (1984).
- ⁷G. Carini, M. Cutroni, M. Federico, and G. Tripodo, *Solid State Ionics* **18/19**, 415 (1986).
- ⁸L. Börjesson, *Phys. Rev. B* **36**, 4600 (1987).
- ⁹L. Börjesson, L. M. Torell, U. Dahlborg, and W. S. Howells, *Phys. Rev. B* **39**, 3404 (1989).
- ¹⁰G. Dalba, P. Fornasini, A. Fontana, F. Rocca, and W. S. Burattini, *Solid State Ionics* **28-30**, 713 (1988).
- ¹¹J. Krogh-Moe, *Phys. Chem. Glasses* **6**, 46 (1965).
- ¹²K. S. Kim and P. J. Bray, *J. Nonmetals* **2**, 95 (1974).
- ¹³J. Krogh-Moe, *Phys. Chem. Glasses* **3**, 1 (1962).
- ¹⁴M. A. Ratner and A. Nitzan, *Solid State Ionics* **28-30**, 3 (1988).
- ¹⁵J. N. Mundy, *Solid State Ionics* **28-30**, 671 (1988).
- ¹⁶N. Bloembergen, E. M. Purcell, and R. V. Pound, *Phys. Rev.* **73**, 679 (1948).
- ¹⁷J. Roos, D. Brinkmann, M. Mali, A. Pradel, and M. Ribes, *Solid State Ionics* **28-30**, 710 (1988).
- ¹⁸J. B. Boyce and B. A. Huberman, *Phys. Rep.* **51**, 189 (1979).
- ¹⁹D. Brinkmann, *Solid State Ionics* **5**, 53 (1981).
- ²⁰D. Brinkmann, *Helv. Phys. Acta* **58**, 167 (1985).
- ²¹P. M. Richards, in *Physics of Superionic Conductors*, edited by M. B. Salamon (Springer, Berlin, 1979), p. 141.
- ²²R. E. Walstedt, R. Dupree, J. P. Remeika, and A. Rodriguez, *Phys. Rev. B* **15**, 3442 (1979).
- ²³G. Villeneuve, P. Echegut, J. M. Reau, A. Levasseur, and J. C. Brethous, *J. Solid State Chem.* **30**, 275 (1979).
- ²⁴J. Senegas, A. M. Villepastour, and C. Delmas, *J. Solid State Chem.* **31**, 103 (1980).
- ²⁵K. Funke and I. Riess, *Z. Phys. Chem. Neue Folge* **140**, 217 (1984).
- ²⁶P. A. Beckmann, *Phys. Rep.* **171**, 85 (1988).
- ²⁷P. M. Richards, *Local Properties at Phase Transitions*, edited by K. A. Muller and A. Rigamonti (North-Holland, Amsterdam, 1976), p. 539.
- ²⁸E. Schweickert, M. Mali, J. Roos, D. Brinkmann, P. M. Richards, and R. M. Biefeld, *Solid State Ionics* **9-10**, 1317 (1983).
- ²⁹J. L. Bjorkstam and M. Villa, *Phys. Rev. B* **22**, 5025 (1980).
- ³⁰K. L. Ngai, in *Non-Debye Relaxation in Condensed Matter*, edited by T. V. Ramakrishnan and M. Raj Lakshmi (World Scientific, Singapore, 1987), p. 23.
- ³¹E. Gobel, W. Muller-Warmuth, and H. Olyschlager, *J. Magn. Reson.* **36**, 371 (1979).
- ³²R. Kohlrausch, *Ann. Phys. (Leipzig)* **12**, 393 (1847).
- ³³G. Williams and D. C. Watts, *Trans. Faraday Soc.* **66**, 80 (1970).
- ³⁴A. K. Jonscher, *Nature* **267**, 673 (1977).
- ³⁵K. L. Ngai, *Comments Solid State Phys.* **9**, 127 (1979).
- ³⁶K. L. Ngai, *Comments Solid State Phys.* **9**, 141 (1980).
- ³⁷R. G. Palmer, D. L. Stein, E. Abrahams, and P. W. Anderson, *Phys. Rev. Lett.* **53**, 958 (1984), and references therein.
- ³⁸A. Blumen, in *Molecular Dynamics and Relaxation Phenomena in Glasses*, edited by Th. Dorfmueller and G. Williams (Springer-Verlag, Heidelberg, 1987), p. 1.
- ³⁹M. Villa and J. L. Bjorkstam, *Solid State Ionics* **9-10**, 1421 (1983).
- ⁴⁰J. L. Bjorkstam, J. Listerud, M. Villa, and C. I. Massara, *J. Magn. Reson.* **65**, 383 (1985).
- ⁴¹H. Looser, D. Brinkmann, M. Mali, and J. Roos, *Solid State Ionics* **5**, 485 (1981).
- ⁴²H. Huber, M. Mali, J. Roos, and D. Brinkmann, *Phys. Rev. B* **37**, 1441 (1988).
- ⁴³R. Kubo and K. Tomita, *J. Phys. Soc. Jpn.* **9**, 888 (1954).
- ⁴⁴A. Abragam, *Principles of Nuclear Magnetism* (Oxford University Press, Oxford, 1961), p. 427.
- ⁴⁵M. Dishon, G. H. Weiss, and J. T. Bendler, *J. Res. Nat. Bur. Stand.* **90**, 27 (1985).
- ⁴⁶K. Funke, *Z. Phys. Chem. Neue Folge* **140**, 251 (1987).
- ⁴⁷K. Funke, *Solid State Ionics* **28-30**, 100 (1988).
- ⁴⁸K. D. Becker and E. Von Goldammer, *Chem. Phys.* **48**, 193 (1980).
- ⁴⁹H. Looser and D. Brinkmann, *J. Magn. Reson.* **64**, 76 (1985).
- ⁵⁰C.-W. Burges, R. Koschmieder, W. Sahn, and A. Schwenk, *Z. Naturforsch. Teil A* **28**, 1753 (1973).
- ⁵¹R. R. Sharp, *J. Chem. Phys.* **60**, 1149 (1974).
- ⁵²D. Brinkmann and W. Freudenreich, *Solid State Commun.* **25**, 625 (1978).
- ⁵³N. Bloembergen and T. J. Rowland, *Phys. Rev. Lett.* **97**, 1679 (1958).
- ⁵⁴Y. Furukawa and Kiriyama, *Chem. Phys. Lett.* **93**, 617 (1982).
- ⁵⁵C. A. Angell, *Solid State Ionics* **18-19**, 72 (1986).
- ⁵⁶H. Fröhlich, in *Theory of Dielectrics* (Oxford University Press, Oxford, 1958).
- ⁵⁷G. Niklasson and L. Börjesson (unpublished).
- ⁵⁸L. Börjesson, L. M. Torell, S. W. Martin, C. Liu, and C. A. Angell, *Phys. Lett. A* **125**, 330 (1987).
- ⁵⁹G. Carini, M. Curtoni, M. Federico, and G. Tripoda, *Phys. Rev. B* **32**, 8264 (1985).